

# Coherent Control of Chemical Reactions

ROBERT J. GORDON\* AND LANGCHI ZHU

*Department of Chemistry (m/c 111), University of Illinois at Chicago, 845 West Taylor Street, Chicago, Illinois 60607-7061*

TAMAR SEIDEMAN

*The Steacie Institute for Molecular Sciences, National Research Council of Canada, Ottawa K1A 0R6, Canada*

Received December 22, 1998

## 1. Introduction

The traditional goals of chemical kinetics are to measure the rates of chemical reactions and to understand their mechanisms on a molecular level. With the advent of lasers and molecular beams, it has become possible to study the reactions of molecules in individual quantum states and to explain their behavior in terms of single collisions governed by well-defined potential energy surfaces. Likewise, numerical methods have been refined to the point that it is possible to predict diverse properties of elementary reactions from first principles. In recent years, the challenge has shifted from measuring and calculating rates of reactions to devising methods of *controlling* their outcome. The idea of controlling the yield and product distribution of a reaction is, of course, a very old one. The field of catalysis, for example, is devoted to finding means of enhancing the natural yield of a reaction. Similarly, temperature and pressure have been used for decades in the chemical industry to alter reaction rates. With the development of narrow-band lasers, it has become possible to excite selectively a single molecular

mode. Provided energy transfer is slow as compared to reaction, such mode-selective preparation of a molecule can be used to alter the outcome of its reaction.<sup>1–3</sup> For example, if the OH bond in HOD is vibrationally excited, that bond becomes more reactive, and collisions with Cl atoms preferentially yield HCl rather than DCl.<sup>4</sup>

A more general, photochemical method for altering reaction pathways exploits the phase property of lasers and has become known as coherent control, or phase control.<sup>5</sup> Two main schemes of coherently controlling physical and chemical processes have been developed over the past decade, based on similar concepts but differing in the properties of the electromagnetic fields that are used. The first, introduced by Tannor and Rice,<sup>6</sup> uses an ultrashort pulse of laser light to create a coherent superposition of energy-resolved eigenstates, namely, a wave packet. Such carefully phased superposition states are, in general, nonstationary. By altering the amplitudes and phases of the light pulses, it is possible to modify the content of the superposition state and thus control the motion of the wave packet. Typically, a vibrational or electronic wave packet is generated at time  $t = 0$  by a short laser pulse. At some later time, when the wave packet has evolved to a desired configuration, a second pulse triggers the reaction. An experimental example of this method is control of the electronic branching ratio of Na atoms in the photodissociation of NaI, which was achieved by varying the timing between two transform-limited ultrashort pulses.<sup>7</sup> Optimal control theory, introduced by Rabitz and co-workers<sup>8</sup> and subsequently developed by several groups,<sup>5</sup> employs a feedback loop to optimize the spectral content and temporal shape of a pulse in order to maximize the yield of a given product. Experimental demonstrations of the control of branching ratios by means of optimally tailored laser pulses were reported by Bardeen et al.<sup>9</sup> and by Assion et al.<sup>10</sup> The use of the intensity property of short pulses to control reactions was also reported.<sup>11</sup>

A second method was introduced by Brumer and Shapiro<sup>12</sup> and is the subject of the present paper. In this approach, two long laser pulses (in principle, they could be continuous beams) excite an atom or a molecule from an initial state to a final state. The frequencies of the lasers are chosen so that the target absorbs either  $m$  photons from the first laser or  $n$  photons from the second laser to reach the same final state.<sup>13</sup> That is, the laser frequencies satisfy the relation  $m\omega_m = n\omega_n$ . An important property of the laser beams is that they have a well-defined phase relation; that is, the phases of the two electromagnetic fields differ by a controllable amount,  $\phi$ . As we will show, by varying the relative phase of the two beams, it is possible to control the branching ratio of the reaction.

It is useful to think of the latter method as an analog of Young's two-slit experiment.<sup>14</sup> In that experiment, particles emerging from two slits create a pattern on a screen. If only one slit is open, the result is a diffraction pattern produced by that slit. If both slits are open,

Robert J. Gordon obtained his doctorate from Dudley Herschbach at Harvard University in 1970. After postdoctoral studies at Caltech and the Naval Research Laboratory, he came to the University of Illinois at Chicago, where he is a professor of chemistry. Prof. Gordon's research interests include experimental studies of the spectroscopy and reaction dynamics of small molecules.

Langchi Zhu received his B.S. from Lanzhou University (P. R. China) in 1985 and his Ph.D. from the State University of New York at Stony Brook in 1994. He joined Robert Gordon's research group at the University of Illinois at Chicago in 1992 as a postdoctoral research associate and became a research assistant professor in 1997. Prof. Zhu's research interests include coherent control of chemical reactions, ion-imaging studies of molecular dynamics and molecular optics, and studies of molecular spectroscopy and intramolecular dynamics using zero-electron-kinetic-energy (ZEKE) pulsed field ionization and mass-analyzed-threshold-ionization (MATI) techniques.

Tamar Seideman received her Ph.D. at the Weizmann Institute of Science in 1990 and did postdoctoral research at the University of California at Berkeley. Since 1993, she has been at the National Research Council in Ottawa, where she is a senior research officer. Prof. Seideman also holds an adjunct professorship at Queens University in Kingston, Ontario. Prof. Seideman's research interests include chemistry and photochemistry at interfaces, molecular dynamics in intense and/or short pulse laser fields, condensed phase dynamics, and the development of mathematical methods.

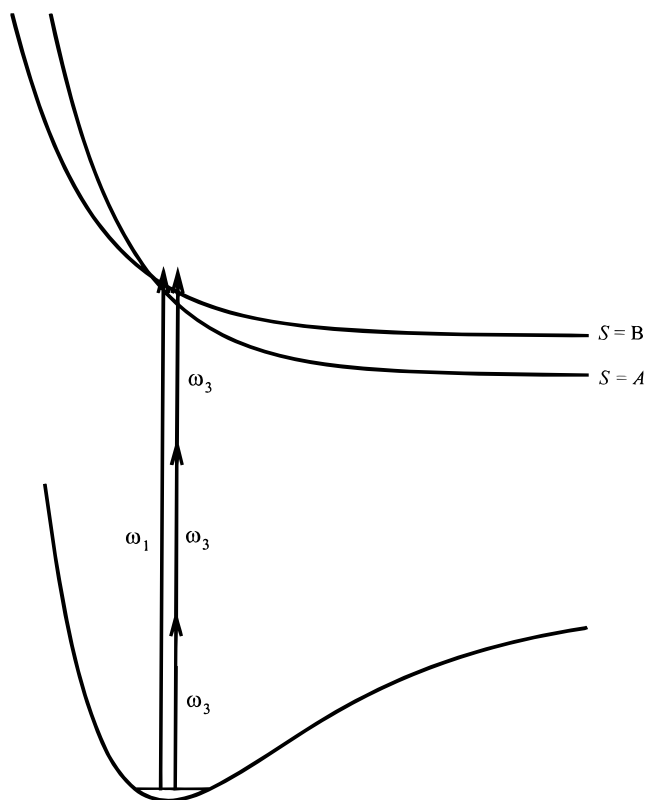


**FIGURE 1.** Schematic illustration of the relation between the scattering potential and the phase of a scattering wave function. The two potential energy curves are illustrations of different dissociative electronic states. Both curves may be reached by either one or three photons ( $n = 1$  and  $m = 3$ ). The different slopes of these curves impart different phases to the outgoing wave functions. These phases are, in turn, responsible for the phases of the transition amplitudes,  $\delta_n$  and  $\delta_m$ . The difference between these phases should not be confused with the phase shift,  $\delta_{13}^S$ , defined by eq 4. See the text for details.

however, an oscillatory pattern results from interference between the waves emerging from each slit. Young's experiment is a useful paradigm for controlling chemical reactions because it shows how properties associated with competing pathways connecting initial and final states interfere with each other. In Young's experiment, waves emerging from the two slits (be they electromagnetic or matter waves) interfere with each other. Similarly, in coherent control experiments, the matrix elements of the two operators connecting the initial and final states (i.e., the transition amplitudes) carry different phases and can thus interfere. In Young's experiment, the phases are determined by the relative positions of the slits and the screen and the refraction index of the medium through which the waves travel, whereas in coherent control they are determined by properties of the molecular target and the laser photon. Importantly, one may *actively control* the relative phase between the two excitation processes by changing the phases of the laser beams.

To understand how control is achieved, consider the reaction probability in the presence of both beams. The key concept is that we do not simply add the transition probabilities for the individual processes. Rather, we add

the two transition *amplitudes* and then square their sum. Assuming, for the moment, that the initial and final states are both bound, the total transition probability is given by<sup>15</sup>

$$p(E) = |p_n(E)^{1/2} + p_m(E)^{1/2} e^{i\phi}|^2 \\ = p_n(E) + p_m(E) + 2(p_n(E)p_m(E))^{1/2} \cos \phi \quad (1)$$

where  $E$  is the total energy,  $p_n$  and  $p_m$  are the transition probabilities for the absorption of  $n$  and  $m$  photons, and  $\phi = m\phi_m - n\phi_n$  is the relative phase of the two electromagnetic fields. Equation 1 shows that the amplitudes for the two excitation paths may interfere constructively or destructively, and that by altering the value of  $\phi$  it is possible to control the product yield.

We consider next the more interesting case where the final state is not bound. That is, we consider reactive processes in which either an electron is ejected from the target or a bond is broken. The occurrence of such reactions introduces three complications. First, because the final state lies in a continuum, its wave function is complex. This property implies that the transition amplitude has a phase,  $\delta_n$  or  $\delta_m$ . Second, if there is more than one product channel, the transition amplitudes and phases are, in general, channel-dependent. We denote this dependence by a channel index,  $S$ . A physical motivation for the channel dependence of the phase is sketched in Figure 1, where the slopes of two continuum potential energy curves give different "kicks" to each product, imparting different phases to the outgoing waves, and hence different values of  $\delta_n$  and  $\delta_m$ . Third, it is necessary to take into account the fact that the reaction products scatter in different directions. Accordingly, we first define a differential transition probability for obtaining product  $S$  at energy  $E$  and scattering vector  $\hat{k}$ ,

$$p^S(E, \hat{k}) = |p_n^S(E, \hat{k})^{1/2} + p_m^S(E, \hat{k})^{1/2} e^{i(\phi + \delta_m^S - \delta_n^S)}|^2 \quad (2)$$

Integrating over scattering angles, we obtain the total transition probability,<sup>15</sup>

$$p^S(E) = p_n^S(E) + p_m^S(E) + 2p_{mn}^S(E) \cos(\phi + \delta_{mn}^S(E)) \quad (3)$$

The *phase shift*,  $\delta_{mn}^S$ , in eq 3 is defined by the expression

$$|p_{mn}^S| e^{i\delta_{mn}^S} = e^{-i\phi} \int d\hat{k} \langle g | D^{(m)} | E S \hat{k}^- \rangle \langle E S \hat{k}^- | D^{(n)} | g \rangle \quad (4)$$

where  $|E S \hat{k}^- \rangle$  is a continuum eigenstate,  $|g \rangle$  is the ground state, and  $D^{(j)}$  is the  $j$ -photon dipole operator.<sup>13</sup> It is worth noting that  $\delta_{mn}^S$  is not equal to  $\delta_m^S - \delta_n^S$ . More importantly, angle integration in eq 4 eliminates much of the interference that is present in the angle-resolved probability given by eq 2. In particular, the coordinate-independent phases, referred to as partial-wave phase shifts in the scattering theory literature<sup>16</sup> and depicted schematically in Figure 1, make no contribution to  $\delta_{mn}^S$ .<sup>17</sup>

There is a subtle but crucial difference between eqs 1 and 3. Equation 1 shows that, for a bound-to-bound transition, the total transition probability can be controlled by varying the laser phase,  $\phi$ . Similarly, eq 3 shows that,

for a reaction with a single product (i.e., where  $S$  can have only one value), one may control the *yield* of the reaction by varying  $\phi$ . For example, the yield of channel A can be maximized by setting  $\phi = -\delta_{mn}^A$ . But, more important, eq 3 shows that the *branching ratio* for forming different products (e.g.,  $S = A$  or  $S = B$ ) may be controlled by varying  $\phi$ . In fact, the branching ratio between different channels can be very sensitive to  $\phi$ , even if the total reaction yield ( $p^A + p^B$ ) varies only weakly with  $\phi$ . From eq 3, it is evident that the branching ratio between channels A and B is controllable if  $\delta_{mn}^A$  and  $\delta_{mn}^B$  differ. A quantity which determines the extent of channel control is the *phase lag*,  $\Delta\delta(A,B)$ , defined as

$$\Delta\delta(A,B) = \delta_{mn}^A - \delta_{mn}^B \quad (5)$$

Although the existence of a phase lag is not a necessary condition to control a branching ratio,<sup>18</sup> it is a definitive signature of control.

Until this point, our emphasis has been on developing tools for controlling the rate and product distribution of a chemical reaction. The phase lag is a new dynamical observable which is well suited for this purpose. To exploit the phase lag for controlling chemical reactions, it is important to discover the underlying molecular properties that determine its value. Our research<sup>17,19–22</sup> has shown that the magnitude of the phase shift for a given channel and its dependence on experimental variables such as energy and mass reflect directly the phases of the scattering wave functions. These phases carry all information about the scattering dynamics. That is, they are determined by the underlying potential energy and are sensitive to subtle features, such as nonadiabatic couplings. The energy dependence of the phase lag, which we denote as “phase lag spectroscopy”, is of fundamental interest, extending far beyond the immediate objective of controlling reactions and providing information that is typically difficult or impossible to calculate *ab initio*.

In what follows, we confine our attention to the case of one- vs three-photon excitation ( $n = 1, 3$ , with laser frequencies  $\omega_1$  and  $\omega_3$  and wavelengths  $\lambda_1$  and  $\lambda_3$ ).<sup>23</sup> In the next section we explain how the phase lag is measured and demonstrate its use to control the branching ratio for the ionization and dissociation of hydrogen iodide. In section 3 we discuss the molecular properties that give rise to a phase lag, and in section 4 we provide some illustrations of phase lag spectroscopy. In the concluding section we return to coherent control, outlining some of the current challenges in the field.

## 2. Experimental Tests of Coherent Control

The key experimental requirements for a coherent control experiment are that (i) the two electromagnetic fields have a well-defined relative phase and (ii) the phase may be varied systematically. The first requirement may be satisfied by using a nonlinear process to generate one field from the other. For example, one may produce the  $\omega_1$  field by focusing a laser beam of frequency  $\omega_3$  into a chamber containing a rare gas such as Xe. Third harmonic genera-

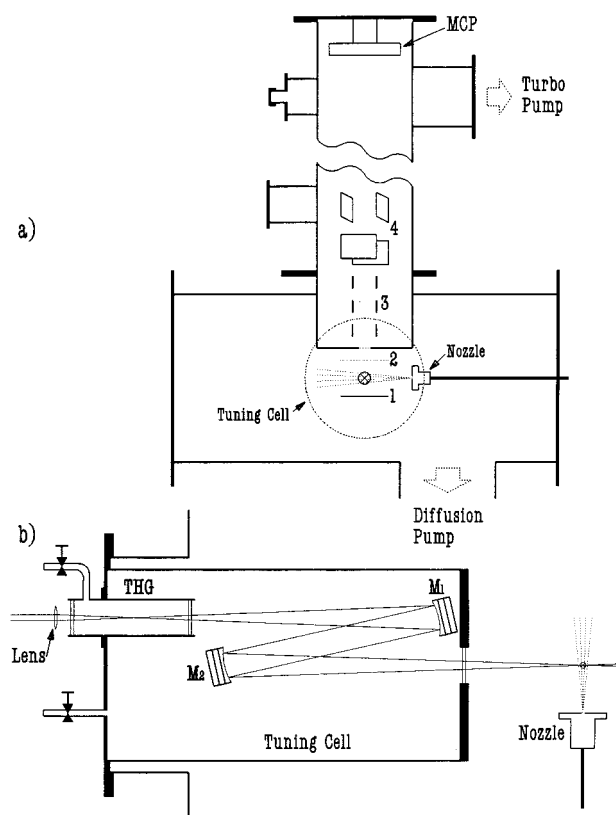


**FIGURE 2.** Schematic drawing of the apparatus, showing the differentially pumped main chamber, time-of-flight tube, microchannel plate (MCP) detector (panel a), and the third harmonic generation (THG) and phase-tuning cells (panel b). In panel a, electrode 1 is the repeller, electrode 2 is the extractor, electrodes 3 are Einzel lenses, and electrodes 4 are steering plates. In panel b, the third harmonic of the UV laser beam is generated in the THG cell, and both laser beams are focused into the main chamber by mirrors  $M_1$  and  $M_2$ .

tion efficiency in the vacuum ultraviolet (VUV) is ca.  $10^{-6}$ – $10^{-5}$ , which is sufficient for this purpose. The second requirement can be met by passing the  $\omega_1$  and  $\omega_3$  beams through a cell containing a gas, such as Ar or  $H_2$ , which has different indices of refraction at the two frequencies. The resulting value of  $\phi$  is proportional to the gas pressure in the phase-tuning cell.<sup>24</sup>

Coherent control experiments may be performed in a reaction cell or in a molecular beam apparatus equipped with a suitable device for detecting the different products. In our apparatus, shown schematically in Figure 2, a molecular beam is injected into a vacuum chamber by a pulsed nozzle, the laser beams are focused into the chamber with a pair of mirrors, and a differentially pumped time-of-flight mass spectrometer is used to detect the product ions.<sup>25</sup>

Early experiments used coherent phase control to transfer population from one bound state to another.<sup>26–30</sup> More challenging, and of greater chemical interest, is the control over bound-to-continuum transitions. To date, coherent control has been demonstrated for the ionization of atoms<sup>31</sup> and molecules,<sup>31,32</sup> the photodissociation of molecules,<sup>33,34</sup> and the switching of photocurrents in semiconductors<sup>35,36</sup> and photocathodes.<sup>37</sup>

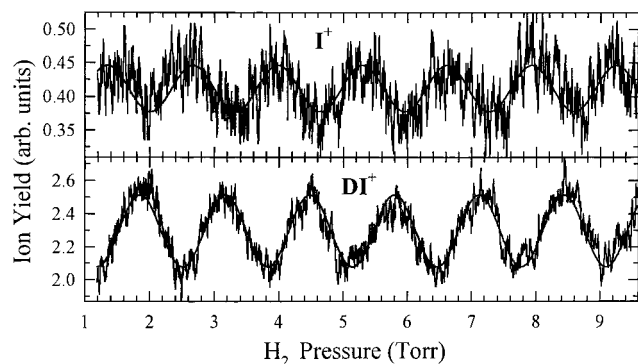


**FIGURE 3.** Modulation of the  $\text{DI}^+$  and  $\text{I}^+$  signals produced by coherent phase control of the photoionization and photodissociation of DI at  $\lambda_1 = 353.69$  nm. The period of the oscillation is determined by the refractive index of  $\text{H}_2$  in the phase-tuning cell. Reprinted with permission from ref 19. Copyright 1997 American Institute of Physics.

An example of coherent control of a branching ratio is shown in Figure 3. In this case, DI molecules are excited just above the ionization threshold with one VUV photon ( $\lambda_1 = 117.90$  nm) and three UV photons ( $\lambda_3 = 353.69$  nm). The two reaction channels are photoionization to produce  $\text{DI}^+$  and photodissociation to produce ground-state D atoms and electronically excited  $\text{I}^*$  atoms. The latter absorb additional photons to yield  $\text{I}^+$ . The  $\text{DI}^+$  and  $\text{I}^+$  signals are recorded as a function of the pressure of  $\text{H}_2$ , which is used as the phase-tuning gas. Figure 3 shows that the ion signals are modulated with the periodicity of  $\phi$ . Also apparent is a phase lag,  $\Delta\delta(\text{DI}^+, \text{I})$ , of  $150^\circ$  between the two channels.

### 3. Physical Origin of the Phase Lag

The observation in Figure 3 that the  $\text{DI}^+$  signal reaches a maximum at a hydrogen pressure where the  $\text{I}^+$  signal is close to a minimum is definitive evidence of coherent control. An intriguing question is the following: What are the physical properties of the system that give rise to the phase lag?<sup>17,19–22,38–40</sup> To appreciate the physical significance of the phase lag, let us consider why  $\delta_{13}^S$  is not exactly zero. A cursory examination of eq 4 might suggest that the phases of the two matrix elements in the integrand should cancel each other out. Specifically, in a one-dimensional world these phases would cancel if the phase of the scattering wave function were coordinate independent. Although the real world is three-dimensional, it is possible, by partial-wave decomposition of  $|\text{ES}\hat{k}^- \rangle$ , to convert the 3D problem into a set of 1D problems, one for each value of the total angular momentum,  $J$ .<sup>17</sup> Upon integration over scattering angles, the interference between different  $J$  states disappears, and a phase shift can arise only from interference between terms of a given  $J$ . In other words, angle integration transforms the problem into the molecular frame, where the existence and energy dependence of a phase shift are directly related to features of the potential energy surface.<sup>17</sup>

Coordinate-independent partial wave phases arise when the continuum potential can induce only elastic

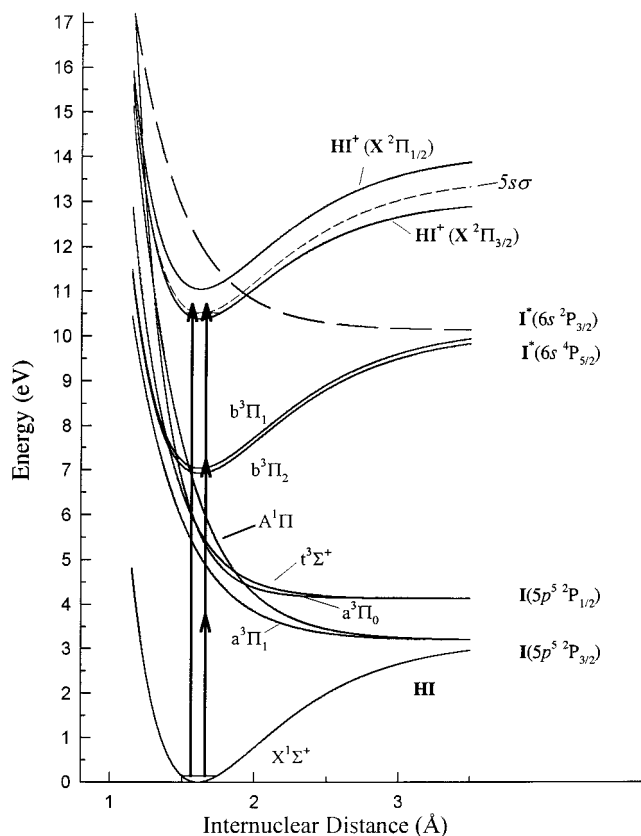


**FIGURE 4.** Potential energy curves involved in controlling the photodissociation and photoionization of HI. The vertical arrows indicate typical energies of the UV and VUV beams. Reprinted with permission from ref 41. Copyright 1995 American Association for the Advancement of Science.

scattering. In this limit, the partial wave radial functions differ from free radial functions only by a phase shift, referred to in the scattering theory literature as the partial wave phase shift and denoted by  $\delta_l$ <sup>16</sup> (not to be confused with  $\delta_{13}^S$  of eq 4). Coordinate independence of the partial wave phase implies that  $p_{13}^S$  is real; that is,  $\delta_{13}^S = 0$  or  $\pi$ . (Examples of *inelastic* potentials for nuclear motion are an angle-dependent potential, which can induce rotational transitions, and a pair of coupled radial potentials, which can mix electronic states.) A sufficient condition for this cancellation *not* to occur is thus that the scattering state that is probed be coupled to some other state. The second state need not necessarily correspond to one of the observed channels. As we shall see later, the large phase lag observed in Figure 3 is direct evidence of exit channel effects in one or both channels. We refer to a phase shift produced by such interactions as a *molecular phase*.

Our experimental studies of the phase lag have focused on the photodissociation and photoionization of HI and DI.<sup>19–21,41,42</sup> To understand the complexities of these processes, it is necessary to examine the potential energy curves lying near  $2\omega_3$  and  $3\omega_3$ , shown in Figure 4. We stress that the potential energy curves of neutral HI at the three-photon level of excitation are not known, and Figure 4 is only schematic. The vertical arrows in Figure 4 indicate excitation of the molecule by either one VUV or



three UV photons from its ground  $X^1\Sigma^+$  state to a continuum lying above the  $X^2\Pi_{3/2}$  state of the ion. The excited molecule can either ionize or dissociate. These reactions may be direct processes, resulting in either prompt emission of an electron or dissociation through a repulsive state to produce electronically excited  $I^*$ .<sup>43</sup> Simultaneously (and coherently), the molecule may be excited by one and three photons into a quasibound resonant state (such as the  $5s\sigma$  Rydberg state shown in Figure 4). The latter undergoes autoionization and predissociation through coupling with the respective continua. Resonant processes such as these are of interest because of their potential for enhancing the reaction yield. They are also likely to have a significant effect on the phase shifts of the different channels. These depend strongly on energy, because the phase of a scattering wave function varies strongly with energy near a resonance.

Figure 4 also shows the presence of two predissociated states ( $b^3\Pi_1$  and  $b^3\Pi_2$ ) that lie near the energy of two UV photons. These states are relevant to the control process because resonances at the two-photon level may contribute a phase to the three-photon path.

The potential energy curves in Figure 4 should not be confused with the heuristic diagram in Figure 1. The latter depicts two dissociative reactions occurring in different electronic states. In Figure 4, one reaction channel corresponds to dissociation on the dashed curve,<sup>43</sup> and the second channel is an ionization reaction that produces  $HI^+(X^2\Pi_{3/2})$ .

The effect of a quasi-bound resonant state on ionization and dissociation was studied many years ago by Fano, who showed that interference between the direct and resonance-mediated pathways to the continuum results in an asymmetric line shape in the absorption spectrum.<sup>44</sup> Assuming, for the moment, that a single photon is absorbed, the amplitudes for the direct and resonance-mediated paths may be denoted, respectively, as  $f_{1d}^S e^{i\delta_{1d}^S}$  and  $f_{1r}^S e^{i\delta_{1r}^S}$ . (Their sum is  $p_m^S(E, \hat{k})^{1/2} e^{i\delta_m^S}$  in eq 2 for  $m = 1$ .) The transition probability is accordingly given by

$$p^S = \int d\hat{k} |f_{1d}^S e^{i\delta_{1d}^S} + f_{1r}^S e^{i\delta_{1r}^S}|^2 \quad (6)$$

This result is mathematically equivalent<sup>17</sup> to the Fano line shape,

$$p^S \propto \frac{(q^{(1)} + \epsilon)^2}{1 + \epsilon^2} \quad (7)$$

where  $q^{(1)}$  is Fano's asymmetry parameter for a one-photon transition, and  $\epsilon$  is a dimensionless energy variable (defined as the offset from resonance divided by half the resonance width).<sup>44</sup>

Equation 6 describes a "two-slit" process without external control. To introduce phase control, we consider the four-slit process depicted in Figure 5, which consists of one-photon direct, one-photon resonance-mediated, three-photon direct, and three-photon resonance-mediated paths. For simplicity we shall refer to them as 1d, 1r, 3d, and 3r paths. In this case, the overall transition

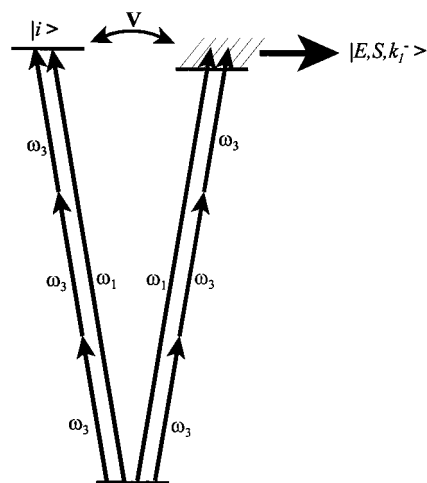


**FIGURE 5.** "Four-slit" mechanism for coherent control. The set of arrows on the right denote direct excitation to the dissociation or ionization continuum. The arrows on the left indicate resonance-mediated paths for either predissociation or autoionization of the molecule.  $V$  is a term in the Hamiltonian that couples the resonance state  $|j\rangle$  to the continuum.

probability for channel  $S$  (ionization or dissociation) is given by

$$p^S = \int d\hat{k} |f_{1d}^S e^{i\delta_{1d}^S} + f_{1r}^S e^{i\delta_{1r}^S} + e^{i\phi} (f_{3d}^S e^{i\delta_{3d}^S} + f_{3r}^S e^{i\delta_{3r}^S})|^2 \quad (8)$$

After integration over scattering angles, four cross terms (1d3d, 1r3r, 1d3r, and 1r3d) contribute to the interference term,  $|p_{13}^S| e^{i\delta_{13}^S}$ , which is a generalization of eq 4.

The transition probability defined by eq 8, and hence also the phase shift as defined in eq 4, may be expressed, by analogy to eq 7, in terms of generalized resonance asymmetry parameters, which, in the most general case, are complex.<sup>22</sup> We do not reproduce the derivation here but only note several limiting results which will be useful in the interpretation of the experimental data presented in the next section:

(i) In the case of a purely elastic scattering potential, in the absence of resonances,  $\delta_{13}^S$  vanishes.

(ii) If an isolated resonance is present and the scattering potential can induce only elastic scattering (i.e., in the absence of a molecular phase),  $|\delta_{13}^S|$  has a *maximum* on resonance and approaches zero at large detunings.

(iii) Irrespective of the nature of the scattering manifold, if an isolated resonance is present and the direct process is negligible compared to the resonance-mediated one, the phase shift vanishes at the resonance energy. In this limit, the excitation and decay processes decouple, and all memory of the excitation scheme is lost once the molecule reacts. An experimental signature of this case is a *minimum* in  $|\delta_{13}^S|$  on resonance, with a nonzero value of the phase lag produced off-resonance by a molecular phase. Overlapping resonances, however, are shown<sup>22</sup> to give rise to a nonzero phase shift, even if a direct route to the continuum is not available.

(iv) Finally, a resonance at an intermediate ( $\omega_3$  or  $2\omega_3$ ) level produces a phase shift even if the continua at the final ( $3\omega_3$ ) level of excitation are structureless and purely elastic. In that case, the phase shift can be shown<sup>22</sup> to

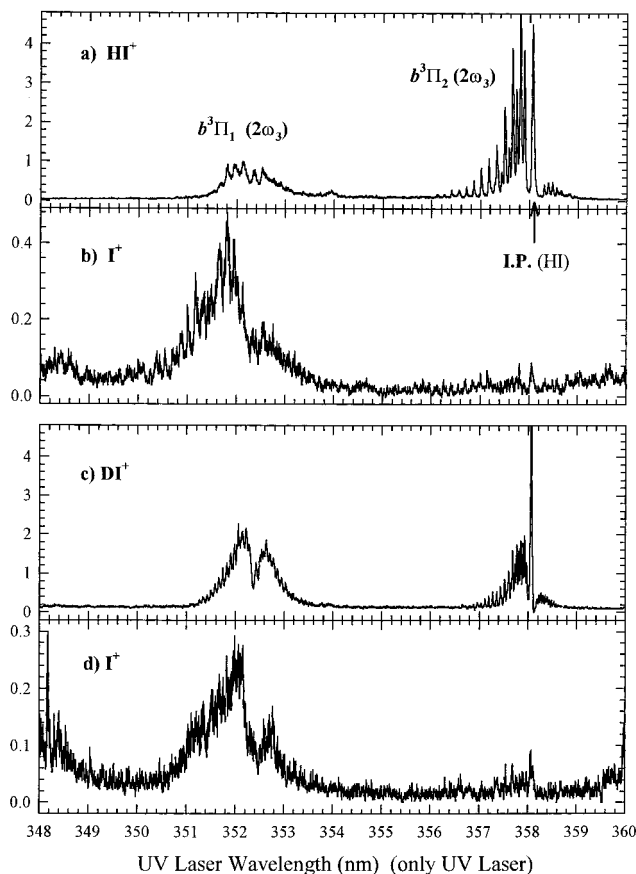


**FIGURE 6.** Resonance-enhanced multiphoton ionization (REMPI) spectra of HI and DI, showing both the parent ions and the neutral iodine atom fragment. The latter is ionized by one or two additional UV photons. The three-photon ionization threshold of HI is indicated by the arrow. Panels a and c show the parent ion signal. Panels b and d show the action spectra of the fragment atom produced by predissociation of the molecule. Reprinted with permission from ref 42. Copyright 1998 Elsevier.

reflect the Breit–Wigner phase<sup>45</sup> associated with the resonance. (See also ref 39.)

#### 4. Phase Lag Spectroscopy of Hydrogen Iodide

The hydrogen iodide molecule is an ideal choice for studying the phase lag between ionization and dissociation for a variety of reasons. First, its low ionization potential makes its ionization continuum easily accessible by tunable third harmonic generation. Second, there are a number of resonant states lying just above the ionization threshold that are coupled to both ionization and dissociation continua. Third, there are two quasi-bound states (the  $b^3\Pi_2$  and  $b^3\Pi_1$  Rydberg states, predissociated by the  $A^1\Pi$ ,  $a^3\Pi_b$ , and  $i^3\Sigma^+$  valence states, shown in Figure 4) lying at approximately two-thirds of the energy of the ionization threshold, which may contribute a phase to the three-photon path.

These properties are visible in the spectra shown in Figures 6 and 7. The presence of the quasi-bound states is evident in the  $2 + 1$  and  $2 + 2$  resonance-enhanced multiphoton ionization (REMPI) spectra shown in Figure 6. Two-photon rotational structure of the  $b^3\Pi_2$  and  $b^3\Pi_1$  states is clearly visible in the molecular ion signals (panels

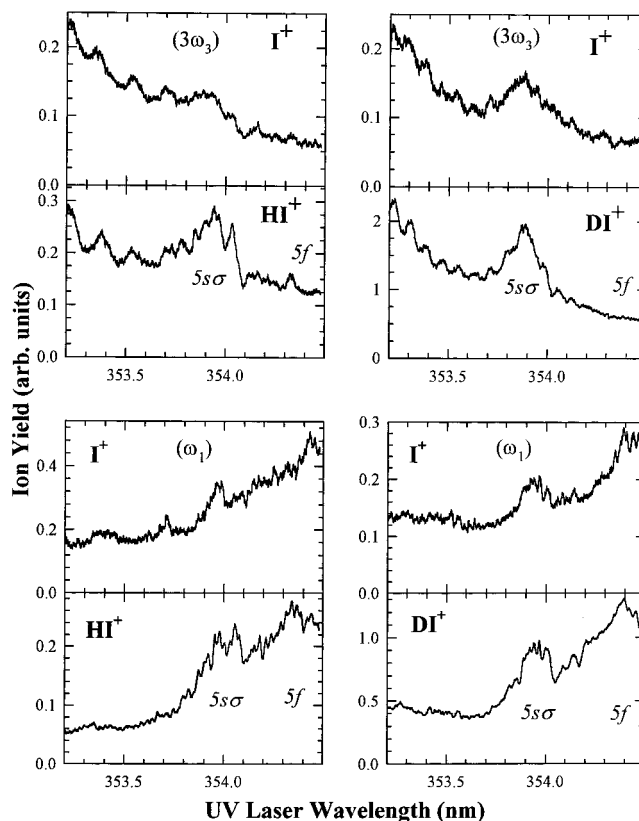


**FIGURE 7.** Three-photon ultraviolet (top four panels) and one-photon vacuum ultraviolet (bottom four panels) spectra of HI and DI, revealing the presence of the  $5s\sigma$  resonance in both the autoionization and predissociation channels. In the two VUV spectra of the I atom fragment, an additional UV photon was used to ionize the product. Reprinted with permission from ref 19. Copyright 1997 American Institute of Physics.

a and c). Predissociation of these states is evident from the  $I^+$  signals shown in panels b and d. The three-photon  $5s\sigma$  resonance is barely visible as a small bump near  $\lambda_3 = 354$  nm. An amplified view of this region of the spectrum is displayed in Figure 7. The four upper panels reveal the presence of the  $5s\sigma$  resonance in the three-photon UV spectra for both autoionization and predissociation of HI and DI. The corresponding one-photon VUV spectra are shown in the bottom four panels. These spectra illustrate that the same resonance, which may be reached by either one or three photons, is embedded in both the ionization and dissociation continua of the molecule.<sup>19</sup>

With these spectra in hand, we proceed to measure the energy dependence of the phase lag. Figure 8 shows  $\Delta\delta(HI^+, I)$  and  $\Delta\delta(DI^+, I)$  in the vicinity of the  $5s\sigma$  resonance. The nonzero phase lag far from the resonance is evidence of exit channel interactions (e.g., interference between different repulsive states) which give rise to the  $1d3d$  term in eq 8. The deep minimum near the resonance is caused by the dominant  $1r3r$  term. As discussed in the conclusion of the previous section (case iii), in the limit where the direct process is negligible compared to the resonance-mediated one (that is, if the continuum is reached only through the isolated resonance), the excitation and decay processes decouple, and the phase shift vanishes.<sup>17</sup> The contribution of the  $1r3d$  and  $1d3r$  interfer-

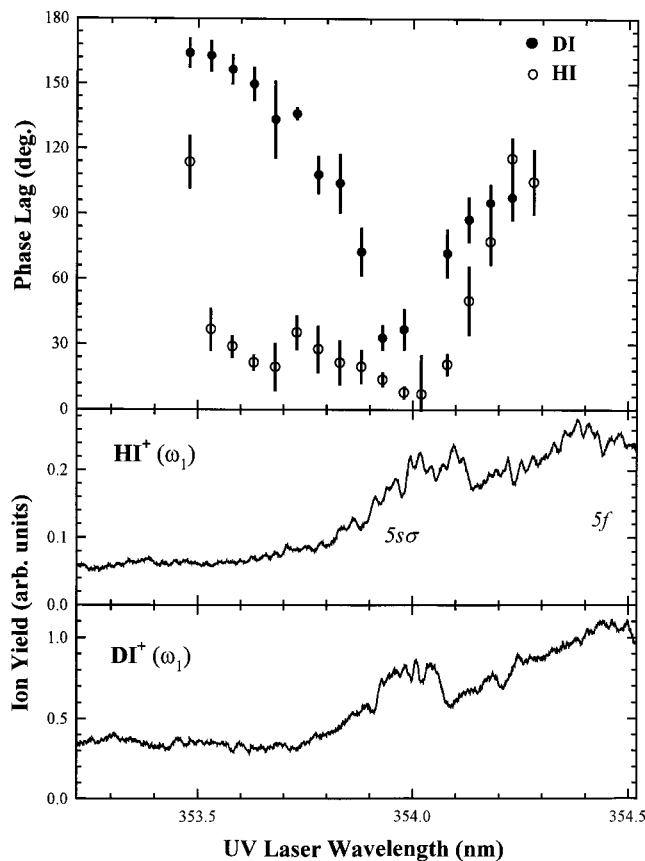


**FIGURE 8.** Phase lag spectrum (top panel) for the photodissociation and photoionization of HI (open symbols) and DI (filled symbols). The bottom two panels give the one-photon photoionization spectra of both molecules, showing the  $5s\sigma$  and  $5f$  autoionizing resonances. Error bars in this and later figures correspond to a single standard deviation. Reprinted with permission from ref 19. Copyright 1997 American Institute of Physics.

ences is dominated by the  $1r3r$  term on-resonance and by the  $1d3d$  term off-resonance.

An interesting question is the following: Which channel (ionization and/or dissociation) is responsible for  $\Delta\delta(\text{HI}^+, \text{I})$  and  $\Delta\delta(\text{DI}^+, \text{I})$ ? Because the phase lag is the difference between two phase shifts, we cannot answer this question from a single measurement. However, by measuring the phase lag between the ionization of HI and DI in a mixture of the two gases, it is possible to assess the contribution of ionization alone. This is true because the difference between the intramolecular phase lags can be rearranged in the form

$$\Delta\delta(\text{HI}^+, \text{I}) - \Delta\delta(\text{DI}^+, \text{I}) = (\delta_{13}^{\text{HI}^+} - \delta_{13}^{\text{DI}^+}) - (\delta_{13}^{1/\text{HI}} - \delta_{13}^{1/\text{DI}}) \quad (9)$$

whereas the phase lag for ionization of the gas mixture is given by

$$\Delta\delta(\text{HI}^+, \text{DI}^+) = \delta_{13}^{\text{HI}^+} - \delta_{13}^{\text{DI}^+} \quad (10)$$

The symbol  $\delta_{13}^{1/\text{HI}}$  in eq 9 denotes the phase shift for the dissociation channel of HI, and likewise for  $\delta_{13}^{1/\text{DI}}$ . The data shown by the squares in Figure 9 demonstrate that  $\Delta\delta(\text{HI}^+, \text{DI}^+)$  vanishes, implying that the ionization channel

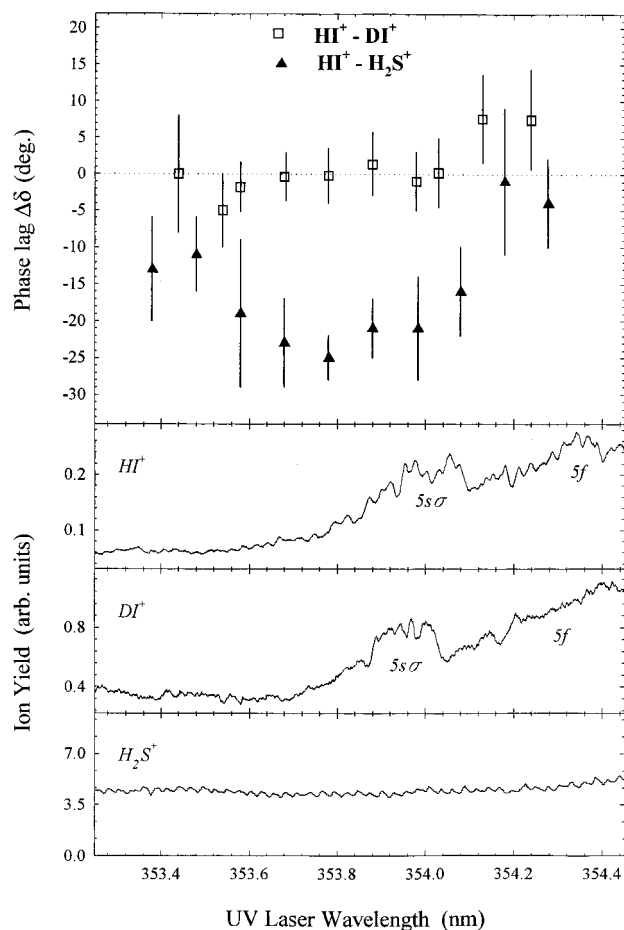


**FIGURE 9.** Phase lag spectrum for the photoionization of a mixture of HI and DI ( $\square$ ) and for the photoionization of a mixture of HI and  $\text{H}_2\text{S}$  ( $\blacktriangle$ ). The bottom three panels show the one-photon (VUV) photoionization spectra of HI, DI, and  $\text{H}_2\text{S}$ . Reprinted with permission from ref 20. Copyright 1999 American Institute of Physics.

does not contribute to the isotope effect in Figure 8. In fact, there is both experimental<sup>20</sup> and theoretical<sup>38,46</sup> evidence that the phase shift for ionization of HI is zero. This result is consistent with our understanding that a phase shift off-resonance is produced by interactions in the continuum.

Assuming that the ionization channel does not contribute a molecular phase, we are now in a position to look for the phase shift that is caused by interferences between the amplitudes for direct and resonant-mediated ( $1r3d$  and  $1d3r$ ) paths. To that end we measured the phase lag between the ionization of HI and a process that has zero phase shift. The direct ionization of  $\text{H}_2\text{S}$  is a convenient choice. Because our spectroscopic measurements showed that the ionization of  $\text{H}_2\text{S}$  has no detectable resonances in the region of interest, we may use the modulated  $\text{H}_2\text{S}^+$  signal as a benchmark against which the absolute phase shifts of other processes, such as the ionization of HI, may be determined. The triangles in Figure 9 show the phase lag for the ionization of a mixture of HI and  $\text{H}_2\text{S}$ ; that is,  $\Delta\delta(\text{HI}^+, \text{H}_2\text{S}^+) = \delta_{13}^{\text{HI}^+}$ . This phase shift reaches a *maximum* in absolute value on resonance, as is expected from the theoretical arguments (case ii) summarized at the end of section 3.

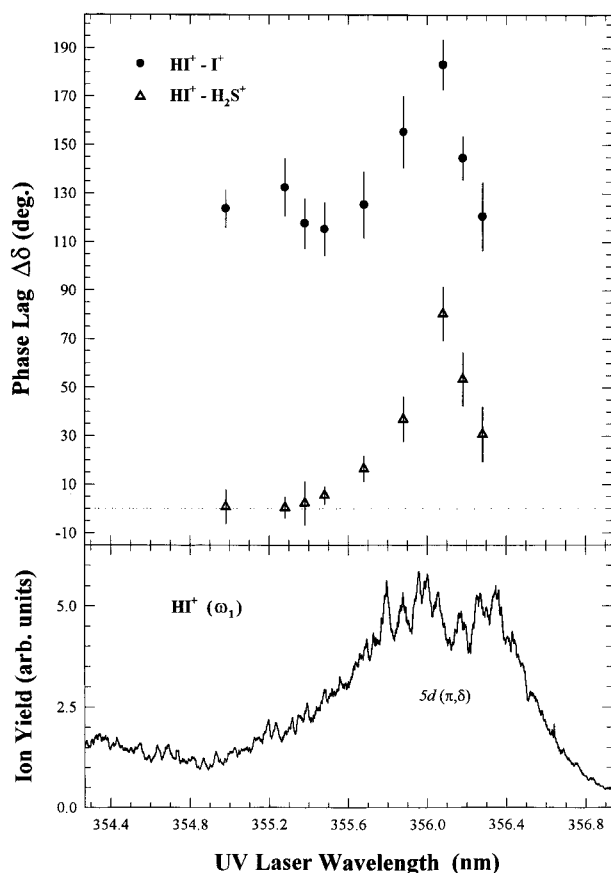


**FIGURE 10.** Phase lag spectrum (top panel) for the photodissociation and photoionization of HI (●) and for the photoionization of a mixture of HI and H<sub>2</sub>S (▲) in the vicinity of the 5d( $\pi,\delta$ ) resonance of HI. The bottom panel is the one-photon ionization spectrum of HI. Reprinted with permission from ref 21. Copyright 1999 The Royal Society of Chemistry.

Still other combinations of the four slits are possible. In Figure 10 are plotted  $\Delta\delta(\text{HI}^+, \text{I})$  and  $\Delta\delta(\text{HI}^+, \text{H}_2\text{S}^+)$  in the vicinity of the overlapping 5d( $\pi,\delta$ ) resonances. Our spectroscopic measurements show that the three-photon resonance peak is absent, indicating that the 3r path vanishes to within our experimental resolution, producing a “three-slit” interference. The ionization phase shift,  $\delta_{13}^{\text{HI}^+} = \Delta(\text{HI}^+, \text{H}_2\text{S}^+)$ , reflects the 1r3d interference alone, whereas the dissociation phase shift,  $\delta_{13}^{\text{HI}^+} = \Delta(\text{HI}^+, \text{H}_2\text{S}^+) - \Delta(\text{HI}^+, \text{I})$ , reflects the 1r3d and 1d3d interferences and is dominated by the latter. Explicit expressions for  $\delta_{13}^{\text{S}}$  in this case are given in ref 22. Finally, in still other experiments we have found evidence of the Breit–Wigner phase produced by rotational resonances at the two-photon level (case iv).<sup>47</sup>

## 5. Future Prospects

The Brumer–Shapiro method of coherent control has by now been demonstrated for many processes and has been tested in considerable detail for HI and DI. The hydrogen iodide measurements extend previous efforts in the field by obtaining control over resonance-mediated reactions. Several issues regarding coherent control are yet to be addressed. The most important one, at least from a chemical perspective, is the selective breaking of different

bonds. There is no reason, in principle, why the methods used to control ionization vs dissociation of HI could not be applied to multiple dissociation continua of small polyatomic molecules. A second issue is the application of coherent control to large polyatomics. In this context, the bound-state control experiments of Wang et al.<sup>28</sup> are encouraging. A third major challenge is the control of collisional processes. Calculations have been published for the D + H<sub>2</sub> reaction,<sup>48</sup> and experiments are awaited.

Much has been said about the possible usefulness of coherent control as a refined chemical tool.<sup>49</sup> Although practical applications of coherent control may eventually be developed, the greatest reward, to date, for pursuing this subject has been the deep insight that it provides toward understanding how the wavelike properties of matter affect photochemical reactions. Our own work has shown that phase lag spectroscopy is not only a valuable tool for controlling chemical reactions but also a powerful method for studying molecular interactions in the continuum.

*It is a pleasure to acknowledge the many graduate students and research associates who have participated in our studies of coherent control, including Ms. Jeanette Allen Fiss, Mr. Toshiyuki Ito, Ms. Ani Khachatryan, Dr. Valeria Kleiman, Dr. Shaoping Lu, Dr. Seung Min Park, Dr. Xiaomei Shi, Mr. Kunihiro Suto, Dr. Karen Trentelman, and Dr. Kaspars Truhins. We particularly wish to thank Prof. Paul Brumer and Prof. Moshe Shapiro for first introducing us to this field and for many helpful discussions during the course of this research. We are grateful to Prof. Michael Trenary, Prof. Timothy Keiderling, and Dr. Kaspars Truhins for critically reading the manuscript. We also wish to acknowledge many valuable interactions with our colleagues, Prof. Masahiro Kawasaki, Prof. Peter Lambropoulos, Prof. H el ene Lefebvre-Brion, Prof. Yutaka Matsumi, and Prof. William Meath. Finally, the generous support of the National Science Foundation is most gratefully acknowledged.*

## References

- (1) Anderson, S. Mode Selective Differential Scattering as a Probe of Polyatomic Ion Reaction Mechanisms. *Acc. Chem. Res.* **1997**, *30*, 28–36.
- (2) Crim, F. F. Vibrationally Mediated Photodissociation: Exploring Excited-State Surfaces and Controlling Decomposition Pathways. *Annu. Rev. Phys. Chem.* **1993**, *44*, 397–428.
- (3) Zare, R. N. Laser Control of Chemical Reactions. *Science* **1998**, *279*, 1875–1879.
- (4) Sinha, A.; Thoemke, J. D.; Crim, F. F. Controlling Bimolecular Reactions: Mode and Bond Selected Reactions of Water with Translationally Excited Chlorine Atoms. *J. Chem. Phys.* **1992**, *96*, 372–376.
- (5) Gordon, R. J.; Rice, S. A. Active Control of the Dynamics of Atoms and Molecules. *Annu. Rev. Phys. Chem.* **1997**, *48*, 601–641.
- (6) Tannor, D. J.; Rice, S. A. Coherent Pulse Sequence Control of Product Formation in Chemical Reactions. *Adv. Chem. Phys.* **1988**, *70*, 441–523.
- (7) Herek, J. L.; Materny, A.; Zewail, A. H. Femtosecond Control of an Elementary Unimolecular Reaction From the Transition-State Region. *Chem. Phys. Lett.* **1994**, *228*, 15–26.
- (8) For a review, see: Rabitz, H.; Kobayahi, T.; Field, R. W.; Tannor, D. J. Ramifications of Feedback Control of Quantum Dynamics. *Adv. Chem. Phys.* **1997**, *101*, 315–325.



- (9) Bardeen, C. J.; Che, J.; Wilson, K. R.; Yakovlev, V. V.; Kohler, B.; Krause, J. L.; Messina, M. Quantum Control of NaI Photodissociation Reaction Product States by Ultrafast Tailored Light Pulses. *J. Phys. Chem. A* **1997**, *101*, 3815–3822.
- (10) Assion, A.; Baumert, T.; Bergt, M.; Brixner, T.; Kiefer, B.; Seyfried, V.; Strehle, M.; Gerber, G. Control of Chemical Reactions by Feedback-optimized Phase-shaped Femtosecond Laser Pulses. *Science* **1998**, *282*, 919–921.
- (11) See, for instance: Szöke, A.; Kulander, K. C.; Bardley, J. N. Simple Calculation of Two-Colour Multiphoton Ionization. *J. Phys. B* **1991**, *24*, 3165. Chelkowski, S.; Bandrauk, A. D.; Corkum, P. B. Efficient Molecular Dissociation by a Chirped Ultrashort Infrared Laser Pulse. *Phys. Rev. Lett.* **1990**, *65*, 2355.
- (12) Brumer, P.; Shapiro, M. Coherence Chemistry: Controlling Chemical Reactions with Lasers. *Acc. Chem. Res.* **1989**, *22*, 407–413.
- (13) In much of the coherent control literature, the notation of nonlinear optics is adopted, where  $\omega_3$ ,  $\lambda_3$ ,  $\delta_3$ , etc. refer to the *one*-photon path, and  $\omega_1$ ,  $\lambda_1$ ,  $\delta_1$ , etc. refer to the *three*-photon path. On the other hand, superscripts have denoted in the previous literature the number of photons absorbed, so that, for example,  $D^{(1)}$  and  $D^{(3)}$  refer, respectively, to one- and three-photon paths. For the sake of clarity, we use in the present paper an unconventional notation in which both sub- and superscripts refer to the number of photons absorbed.
- (14) Tonomura, A.; Endo, J.; Matsuda, T.; Kawasaki, T. Demonstration of Single-Electron Buildup of an Interference Pattern. *Am. J. Phys.* **1989**, *57*, 117–120.
- (15) Brumer, P.; Shapiro, M. Coherent Radiative Control of Unimolecular Reactions. *Faraday Discuss.* **1986**, *82*, 177–185.
- (16) Newton, R. G. *Scattering Theory of Waves and Particles*; McGraw-Hill Book Co.: New York, 1966.
- (17) Seideman, T. The Role of a Molecular Phase in Two-Pathway Excitation Schemes. *J. Chem. Phys.* **1998**, *108*, 1915–1923.
- (18) Gordon, R. J.; Fiss, J. A.; Zhu, L.; Seideman, T. Coherent Phase Control of Photoionization and Photodissociation. In *Coherent Control in Atoms, Molecules, and Semiconductors*; Pötz, W. A., Schroeder, W. A., Eds.; Kluwer: Dordrecht, 1999; pp 39–49.
- (19) Zhu, L.; Suto, K.; Fiss, J. A.; Wada, R.; Seideman, T.; Gordon, R. J. The Effect of Resonances on the Coherent Control of the Photoionization and Photodissociation of HI and DI. *Phys. Rev. Lett.* **1997**, *79*, 4108–4111.
- (20) Fiss, J. A.; Zhu, L.; Gordon, R. J.; Seideman, T. The Origin of a Phase Lag in the Coherent Control of Photoionization and Photodissociation. *Phys. Rev. Lett.* **1999**, *82*, 65–68.
- (21) Fiss, J. A.; Zhu, L.; Gordon, R. J.; Seideman, T. The Role of Molecular and Resonance Phases in the Coherent Control of Chemical Reactions. *Discuss. Faraday Soc.* **1999**, *113*, 61–75.
- (22) Seideman, T. Phase-Sensitive Observables as a Route to Understanding Molecular Continua. *J. Chem. Phys.* **1999**, *111*, 9168–9182.
- (23) Shapiro, M.; Hepburn, J. W.; Brumer, P. Simplified Laser Control of Unimolecular Reactions: Simultaneous  $(\omega_1, \omega_3)$  Excitation. *Chem. Phys. Lett.* **1988**, *149*, 451–454.
- (24) Gordon, R. J.; Lu, S.; Park, S. M.; Trentelman, K.; Xie, Y.; Zhu, L.; Kumar, A.; Meath, W. J. The Use of Coherent Phase Control of Multiphoton Ionization to Measure the Refractive Indices of H<sub>2</sub> and Ar Between 1100 and 1150 Å. *J. Chem. Phys.* **1993**, *98*, 9481–9486.
- (25) Lu, S.; Park, S. M.; Xie, Y.; Gordon, R. J. Coherent Laser Control of Bound-to-Bound Transitions of HCl and CO. *J. Chem. Phys.* **1992**, *96*, 6613–6620.
- (26) Chen, C.; Yin, Y. Y.; Elliott, D. S. Interference between Optical Transitions. *Phys. Rev. Lett.* **1990**, *64*, 507–510.
- (27) Park, S. M.; Lu, S. P.; Gordon, R. J. Coherent Laser Control of the Resonantly Enhanced Multiphoton Ionization of HCl. *J. Chem. Phys.* **1991**, *94*, 8622–8624.
- (28) Wang, X.; Bersohn, R.; Takahashi, K.; Kawasaki, M.; Kim, H. L. Phase Control in Large Polyatomic Molecules. *J. Chem. Phys.* **1996**, *105*, 2992–2997.
- (29) Fiorini, C.; Charra, F.; Nunzi, J. M.; Samuel, I. D. W.; Zyss, J. Light-Induced Second-Harmonic Generation in an Octopolar Dye. *Opt. Lett.* **1995**, *20*, 2469–2471.
- (30) Karapanagioti, N. E.; Xenakis, D.; Charalambidis, D.; Fotakis, C. Coherent Control in Four-Photon Excitation Schemes. *J. Phys. B* **1996**, *29*, 3599–3609.
- (31) Yin, Y. Y.; Chen, C.; Elliott, D. S. Asymmetric Photoelectron Angular Distributions from Interfering Photoionization Processes. *Phys. Rev. Lett.* **1992**, *69*, 2353–2356.
- (32) Kleiman, V. D.; Zhu, L.; Li, X.; Gordon, R. J. Coherent Phase Control of the Photoionization of H<sub>2</sub>S. *J. Chem. Phys.* **1995**, *102*, 5863–5866.
- (33) Kleiman, V. D.; Zhu, L.; Allen, J.; Gordon, R. J. Coherent Control Over the Photodissociation of CH<sub>3</sub>I. *J. Chem. Phys.* **1995**, *103*, 10800–10803.
- (34) Sheehy, B.; Walker, B.; DiMauro, L. F. Phase Control in the Two-Color Photodissociation of HD<sup>+</sup>. *Phys. Rev. Lett.* **1995**, *74*, 4799–4802.
- (35) Dupont, E.; Corkum, P. B.; Liu, H. C.; Buchanan, M.; Wasilewski, Z. R. Phase-Controlled Currents in Semiconductors. *Phys. Rev. Lett.* **1995**, *74*, 3596–3599.
- (36) Hachè, A.; Kostoulas, Y.; Atanasov, R.; Hughes, J. L. P.; Sipe, J. E.; van Driel, H. M. Observation of Coherently Controlled Photocurrent in Unbiased, Bulk GaAs. *Phys. Rev. Lett.* **1997**, *78*, 306–309.
- (37) Zel'dovich, B. Ya.; Chudinov, A. N. Interference of Fields with Frequencies  $\omega$  and  $2\omega$  in External Photoelectric Effect. *Sov. Phys. JETP Lett.* **1989**, *50*, 439–441.
- (38) Lefebvre-Brion, H. Study of the Origin of the Phase Lag Between Signals in Coherent Laser Control. *J. Chem. Phys.* **1997**, *106*, 2544–2546.
- (39) Lee, S. On the Molecular Phase in Coherent Control. *J. Chem. Phys.* **1997**, *107*, 2734–2737.
- (40) Lambropoulos, P.; Nakajima, T. Origin of the Phase Lag in the Modulation of Photoabsorption Products under Two-Color Fields. *Phys. Rev. Lett.* **1999**, *82*, 2266–2269.
- (41) Zhu, L.; Kleiman, V. D.; Li, X.; Lu, S.; Trentelman, K.; Gordon, R. J. Coherent Laser Control of the Product Distribution Obtained in the Photoexcitation of HI. *Science* **1995**, *270*, 77–80.
- (42) Fiss, J. A.; Zhu, L.; Suto, K.; He, G.; Gordon, R. J. Mechanism of the Coherent Control of the Photoionization and Photodissociation of HI and DI. *J. Chem. Phys.* **1998**, *233*, 335–342.
- (43) Although the symmetry of the dissociative state is unknown, an analogous curve for HCl has been assumed to have 3Π<sub>0</sub> symmetry, on the assumption

- that it is the lowest of a Rydberg series converging to the  $a^4\Pi$  ion core. See: Lefebvre-Brion, H.; Keller, F. Competition Between Autoionization and Predissociation in the HCl and DCl Molecules. *J. Chem. Phys.* **1989**, *90*, 7176–7183.
- (44) Fano, U. Effect of Configuration Interaction on Intensities and Phase Shifts. *Phys. Rev.* **1961**, *124*, 1866–1878.
- (45) Sakurai, J. J. *Modern Quantum Mechanics*; Addison-Wesley: Reading, MA, 1994.
- (46) Althorpe, S. C.; Seideman, T., unpublished results.
- (47) Fiss, J. A.; Khachatria, A.; Truhins, K.; Zhu, L.; Gordon, R. J.; Seideman, T. Direct Observation of the Breit-Wigner Phase in the Coherent Control of the Photoionization of HI. (submitted).
- (48) Abrashkevich, A.; Shapiro, M.; Brumer, P. Coherent Control of Reactive Scattering. *Phys. Rev. Lett.* **1998**, *81*, 3793–3796.
- (49) Brumer, P.; Shapiro, M. Laser Control of Chemical Reactions. *Sci. Am.* **1995**, March, 34–39.

AR970119L